PHOTOVOLTAIC EFFECTS

Photovoltaic devices convert light into electricity. The photovoltaic effect was first observed in 1839 by the French physicist Becquerel, who reported that the uneven illumination of two identical electrodes in a conducting solution produced electricity. Following Smith's observation that the conductivity of selenium is higher during exposure to light (the first discovery of the photoconductivity effect), Adams and Day reported a photovoltaic effect in gold-coated selenium and built the first photovoltaic photocell in 1876. The implications for power generation have spurred recent work in photovoltaics (see SOLAR CELLS). Here we describe the signal information aspect of the photovoltaic effect and photovoltaic devices that measure such quantities as the magnitude and position of incident light. Two distinct photovoltaic effects are exploited for photovoltaic devices: the transverse photovoltaic effect and the lateral photovoltaic effect. The transverse photovoltaic effect is more commonly cited and is used in such devices as photodiodes for detecting the magnitude of low light levels. The lateral photovoltaic effect is more subtle but is sensitive to the location and spatial variation of illumination. This effect has been used to manufacture position-sensitive detectors that return a voltage varying continuously with the position of an incident light spot.

TRANSVERSE PHOTOVOLTAIC EFFECT

Photovoltaic devices usually are constructed from semiconductors, which have moderate conductivities between the low conductivities of insulators and the high conductivities of metals. Semiconductors are chosen for photovoltaic and other electronic applications because this conductivity can be tightly controlled by manufacturing processes and is very responsive to external stimuli such as applied electric fields or incident light, as described in what follows.

A semiconductor such as crystalline silicon exists in a regular periodic formation called a lattice, held together by covalent bonding between the four valence electrons of each neighboring silicon atom. One of these covalent bonds may break when a photon of sufficiently energetic light hits this silicon lattice, freeing an electron to roam the crystal. Because an electron near the broken bond may move from its bond to the newly created vacancy, leaving a new vacancy behind, the vacancy (called a hole) also roams the crystal. A hole (absence of an electron) moves about the lattice in the same way a bubble (absence of liquid) moves in a liquid. When an electron and hole are generated by this absorption of a photon, we say that the photon 'creates' the electron-hole pair.

The periodic lattice structure of crystalline silicon causes interactions between the discrete energy levels of the constituent silicon atoms that merge the discrete atomic energy levels into discrete energy bands. These discrete bands are separated by forbidden gaps. Electrons may only have those energies represented by the bands; they may not possess any value of energy within the forbidden gap. The photoelectrical action in a semiconductor takes place in the valence band, which is mostly full of electrons, and the conduction band above it, which is mostly empty of electrons. In this band picture, when a photon creates an electron-hole pair, an electron is promoted from the valence band to the conduction band as shown in Fig. 1. Note that a hole is simultaneously created in the valence band.

Ordinarily, these charge carriers, electrons, and holes, will recombine or be captured by defect centers. To get any electricity out of a photovoltaic device, these electrons and holes must be segregated from each other before any trapping or

J. Webster (ed.), *Wiley Encyclopedia of Electrical and Electronics Engineering*. Copyright © 1999 John Wiley & Sons, Inc.

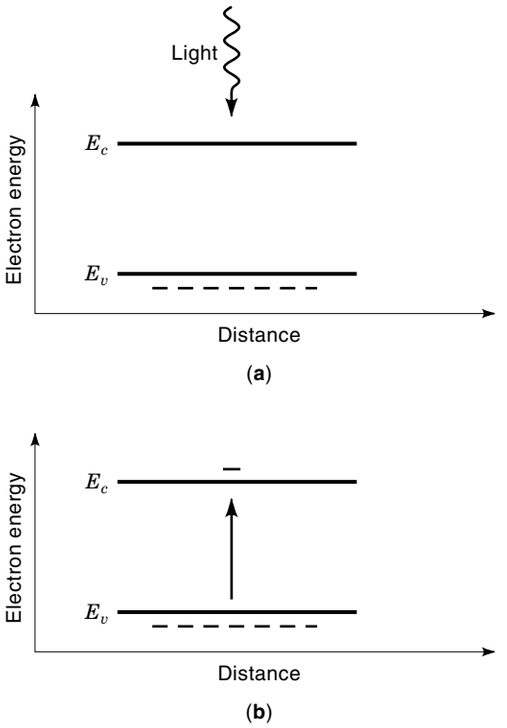

Figure 1. Band picture of photon absorption in bulk semiconductor. (a) Band picture before absorption. (b) After absorption, an electron is promoted from the valence band to the conduction band.

recombination occurs; otherwise, the absorbed light merely serves to heat the semiconductor. If light generates an electron-hole pair near an internal potential gradient, then the pair can separate; the negatively charged electron moves toward the positive potential while the hole (like a positively charged particle) moves opposite. If there are contacts on the device, one on each side of the internal potential gradient, then these contacts will develop a voltage. The contact on the region containing the holes will be positive with respect to the contact on the region containing the electrons. Equilibrium between the voltage developed at the contacts and the counteracting internal potential results in an open circuit voltage. If these contacts are electrically connected to an outside circuit then the recombination of photogenerated electrons and holes via this external path gives rise to a current flow.

The internal potential gradient can be formed in the semiconductor during manufacture by doping, which is the controlled addition of specific impurities to the semiconductor. Following is a brief description of the band bending in a silicon p–n junction without any illumination or applied voltage. The n-type side of the junction contains 'donor' atoms such as arsenic that are thermally ionized, leaving positively charged impurity sites fixed in their locations. These impurities donate their extra electrons which circulate as majority carriers; hence this material is called n-type. The p-type side of a silicon p–n junction contains thermally ionized 'acceptor' atoms such as boron, leaving negatively charged sites also fixed in place. The impurities on the p-type side accept electrons, leaving holes as majority carriers. At thermal equilibrium and zero applied voltage there is no net current, so the net motion of charge carriers due to drift (from internal electric fields) just equals that due to diffusion (random redistribution of charge carriers from regions of higher concentration to regions of lower concentration). To reach equilibrium a space charge region forms around the junction, with a charge distribution governed by the Poisson equation. The p-side of the space-charge region is depleted of free holes, leaving behind fixed negative charge. Similarly, the n-side of the space-charge region is depleted of free electrons, leaving behind fixed positive charge. As shown in Fig. 2, this space charge region induces band bending around the junction. The Fermi level E_F represents the energy at which the probability of electron occupation is exactly one-half; in the band-banding diagram any shift in E_F represents the external voltage between the ends of the device. Since there is no applied voltage or external illumination on the device, the Fermi level E_F is flat in Fig. 2(c).

Now consider what happens when this structure is illuminated by light sufficiently energetic to create electron-hole pairs. Suppose the light impinges on the p-side, as shown in Fig. 2(d), and creates electron-hole pairs in the p-layer. If this creation process occurs near enough (within a minority carrier diffusion length) to the junction such that some electrons reach the junction before being lost to recombination, then these electrons will be swept across the junction into the n-region, separating them from the holes that remain in the p-layer. These electrons are attracted by the fixed positive charge on the n-side of the junction. This separated charge now cancels some of the junction space charge, reducing the band bending and developing an external potential as depicted by the shift φ in the Fermi level E_F. If external contacts are present at both ends of this device, then a voltage can be measured and current delivered to an external circuit. Note that the theoretical maximum voltage that can be delivered from a single p–n junction is just the amount needed to flatten the conduction and valence bands, which is called the built-in voltage of the junction. This cannot exceed the bandgap ($E_c - E_v$), a fixed property of the semiconductor. Higher voltages can be obtained by connecting multiple p–n junctions in series. This has been proposed to occur at the microscopic level through stacking faults in materials such as ZnS and ZnSe, which are observed to produce net photovoltages up to several hundred volts.

Applications

The most common photovoltaic sensor based on the transverse photovoltaic effect is the simple photodiode. Photodiodes may be constructed from homojunctions (between differently doped areas of the same semiconductor material) such as the p-n junctions described previously. They are also fabricated from junctions between dissimilar materials, such as a heterojunction (between two different semiconductors) or a Schottky barrier (metal-semiconductor junction). Photodiodes are most commonly operated under reverse bias, which increases the potential gradient acting on the photogenerated carriers. This higher field decreases carrier transit time from the illumination point to the contacts, reducing junction capacitance and thus allowing higher operating speeds. However, the unbiased photovoltaic mode of operation is more sensitive to low light levels, since in the dark there is only thermal noise and no dark current to compete with the photocurrent.

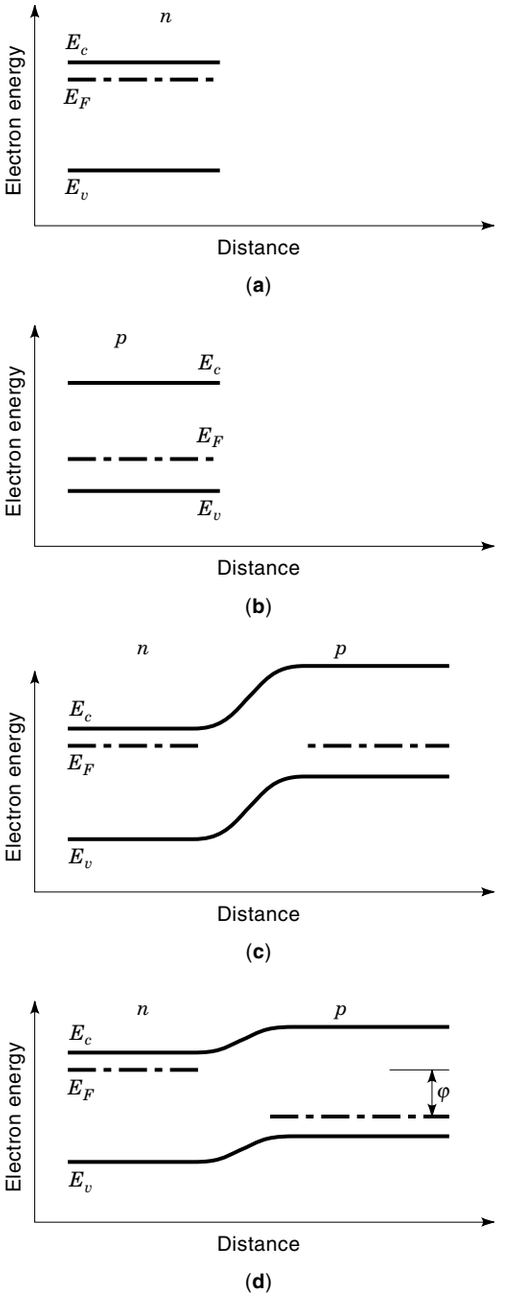

Figure 2. The transverse photovoltaic effect. (a) *n*-type bulk semiconductor, with Fermi level near the conduction band. (b) *p*-type bulk semiconductor. (c) *p–n* junction, showing band bending required to line up the Fermi levels in the two sides of the junction. (d) *p–n* junction under illumination, where the photogenerated charge has reduced the band bending by the photovoltage φ.

The photovoltaic effect in a *p–n* junction photodiode is well-known. The device current I is approximately related to the photovoltage φ by

$$I = I_s(e^{q\varphi/k_b T} - 1) - I_L \tag{1}$$

where I_s is the diode saturation current, q is the charge of the electron, k_b is the Boltzmann constant, T is the absolute temperature, and I_L is the photogenerated current which is proportional to the illuminance. From this we can see that while the open-circuit voltage [when $I = 0$ in Eq. (1)] varies inconveniently with the temperature and the log of illuminance, the short-circuit current [when $\varphi = 0$ in Eq. (1)] is linear with illuminance and is basically temperature-independent. Therefore, for a linear response, photodiodes operated in a photovoltaic mode are connected to a current amplifier as shown in Fig. 3 which provides an output voltage proportional to the short-circuit device photocurrent. In addition to improved linearity, operating in a short-circuit mode improves the frequency response by reducing capacitive charging of the photodiode.

Photodiode arrays such as the DPSD-2064 manufactured by EG&G Heimann Optoelectronics (1) can perform pattern detection and position sensing. This device contains a square array of 64 × 64 elements in an active area 2 cm × 2 cm, and is sensitive throughout the visible spectrum, from 400 nm to 800 nm. The device is constructed from a thin layer of amorphous silicon between two layers that each contains parallel rows of semitransparent electrode stripes. The stripes on the bottom layer are oriented perpendicular to those on the top layer, so that the photocurrent from each individual photodiode can be measured in turn. When used to detect the position of an incident light spot that covers several elements, accuracy better than the actual resolution of the array can be achieved by calculating the centroid of the measured photovoltages. EG&G Heimann Optoelectronics sells an accompanying signal processing board that will perform this centroid calculation and other functions such as tracking and full array readout.

Photovoltaic-based optoisolators can be built using a photovoltaic driver electrically connected to the gate of a metal-oxide-semiconductor field-effect transistor (MOSFET). Multiple photovoltaic elements in series can generate several volts at low current levels, which is just what the gate of a MOSFET requires to allow current flow from source to drain. This arrangement, when encapsulated with a light emitting diode (LED), forms a photovoltaic optoisolator that behaves like a relay (2). A conventional optoisolator may contain an LED illuminating the base of a phototransistor, which requires power and additional circuitry on the output side to bias the phototransistor. Using a photovoltaic element to provide the gate current for a MOSFET eliminates the need for load side bias while retaining electrical isolation between the driving signal and the load. Such solid state switches have advan-

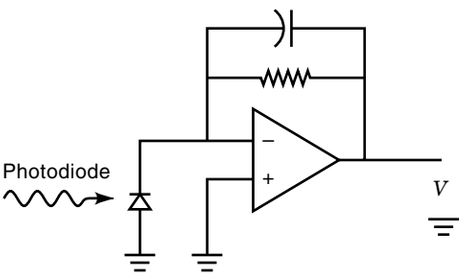

Figure 3. Current to voltage amplifier for a photodiode operated in the photovoltaic mode. The output voltage V is proportional to the short-circuit photocurrent, which is linear with illuminance. The capacitor provides phase compensation.

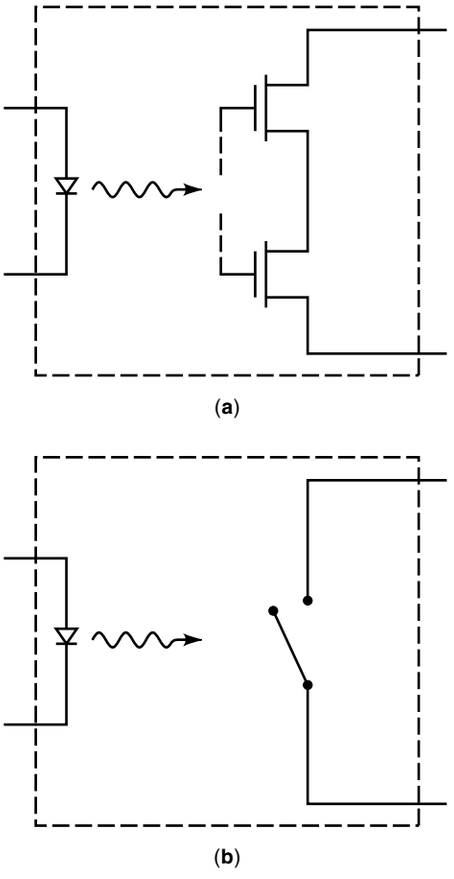

Figure 4. Solid state relay. (a) Encapsulated LED activates MOSFET gates. (b) Ideal equivalent circuit.

tages over electromechanical relays, such as faster response, less noise, and low activation currents that are directly compatible with computer interfaces.

Hewlett Packard (3) manufactures a series of similar optoisolator solid-state relays which function as normally-off single-pole bi-directional relays as shown in Fig. 4. For the HSSR-8200, the input LED requires at least 1 mA and 1.85 V. The output MOSFETs have an off-resistance of 10 TΩ and an on-resistance of 100–160 Ω. At an input LED current of 5 mA the MOSFET switching times are about 50 μS; the switching times are somewhat longer at lower LED currents. This device provides isolation between input and output of up to 2500 Vac. Other devices in this family trade-off performance in various ways; for example, the HSSR-8060 features MOSFET on-resistance of just 0.4 Ω, but requires an increased LED input current of 10 mA.

LATERAL PHOTOVOLTAIC EFFECT

Schottky first reported the lateral photovoltaic effect in 1930 in a study of Cu-Cu_2O metal-semiconductor junctions, but his finding was forgotten until 1967, ten years after Wallmark's 1957 rediscovery of the effect. The lateral photovoltaic effect coexists with the transverse photovoltaic effect already described. Consider a p–n junction locally illuminated by a spot of light, that is, the light spot hits only part of the p-n junction leaving the rest dark. The junction separates the photoinduced charge carriers as described above for the transverse photovoltaic effect. In addition, the diffusion process (whereby charge carriers tend to redistribute from regions of high concentration to regions of lesser concentration) acts to move carriers laterally away from the illuminated part of the device toward the dark areas. As the charges diffuse outward, a fraction recombine transversely back across the junction, creating a tapered charge distribution as depicted in Fig. 5(a). This junction leakage current robs the lateral diffusion current as depicted in Fig. 5(b). The Fermi level shift and accompanying band bending directly under the light spot are shown in Fig. 5(c), where the separated charge reduces the internal barrier. This is just the transverse photovoltaic effect. Further out, in a dark area of the device adjacent to the illumination, the separated charge present is only that which has diffused from the illuminated area, so the shift of the band bending is less as shown in Fig. 5(d). Thus, the induced photovoltage is maximum under the illumination and falls off with distance from the light spot.

As long as the illumination continues, the charges generated by the light diffuse outward and eventually recombine some distance away. In steady-state, current continuity implies that the transverse recombination current will equal the rate of photoinduced charge separation. The presence of the separated charge before recombination reduces the internal potential, creating a potential deviation that decreases with radial distance from the light spot. Typically, one side of the junction is more highly doped, which is then treated as an equipotential surface. A pair of ohmic contacts are then placed on the less doped side, which will measure the difference in the transverse photovoltages at their locations. Now consider what happens when a light spot sweeps from one contact toward the other. As shown in Fig. 6, when the light spot is in the center between the two contacts, the system is symmetrical and the photovoltage is zero. When the light spot moves closer to one contact, a voltage develops; when the light spot moves closer to the other contact, the voltage has the opposite polarity. This then is a rudimentary position-sensitive detector, for which a light spot position can be determined to 100 Å or 0.1 second of arc. Since the voltage crosses zero at center, bridge or null methods can be used to obtain extreme accuracy. Position-sensitive detectors based on the lateral photovoltaic effect have no insensitive areas, unlike the photodiode array described above. Although illustrated here for a p–n junction, the effect is present in any nonuniformly illuminated junction between two materials of differing conductivities, including p–p^+ junctions, Schottky barriers, grain boundaries, and others. Figure 7 summarizes the measurement configurations for both the transverse photovoltaic effect and the lateral photovoltaic effect.

Lucovsky (4) gives the basic equations describing the lateral photovoltaic effect. For an n^+–p junction we can take the n^+ region as equipotential. If we illuminate this junction locally with a light spot, creating electron hole pairs that are separated by the junction, the lateral current flow $J_L(r)$ in the p region at radius r follows the transverse photovoltage $\varphi(r)$ as

$$\frac{d\varphi(r)}{dr} = -\rho J_L(r) \tag{2}$$

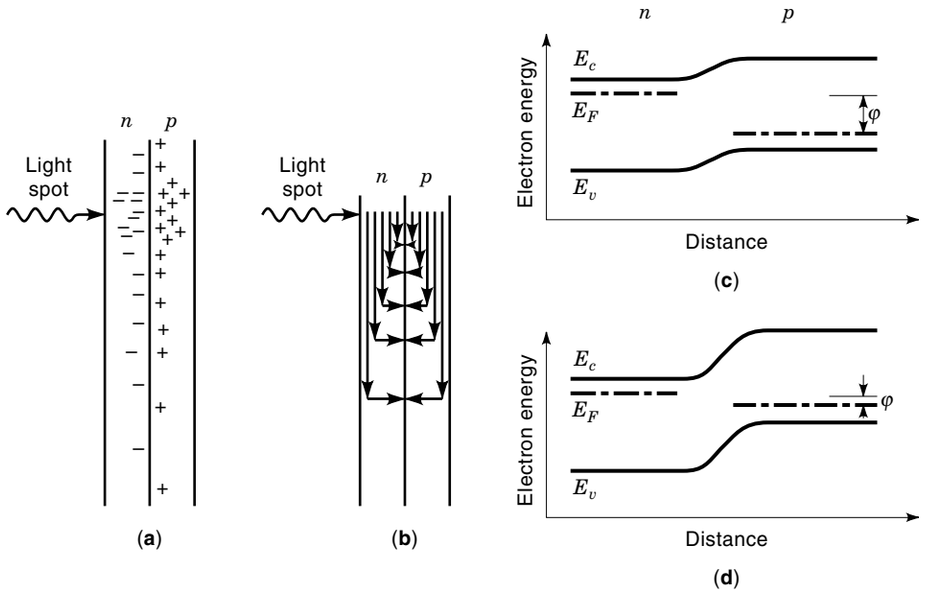

Figure 5. (Not to scale) Lateral photovoltaic effect in steady state. (a) Photogenerated charge carriers are separated by the junction and diffuse away. (b) Arrows show the net motion of the charge carriers. The lateral diffusion photocurrent is robbed by recombination back across the junction. (c) The bands at the junction directly under the light spot flatten due to the transverse photovoltaic effect. (d) Reduced flattening of the bands some distance from the light spot, induced by the laterally diffused photoinduced charge not yet recombined.

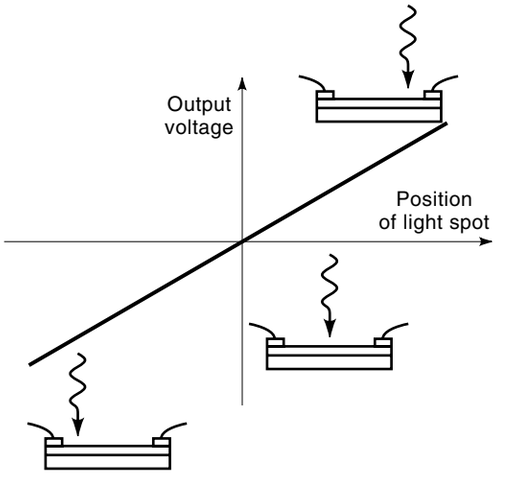

Figure 6. Output voltage varies with position of light spot for a position-sensitive detector. Note that the photovoltage changes polarity when the light spot crosses the center, due to configuration symmetry.

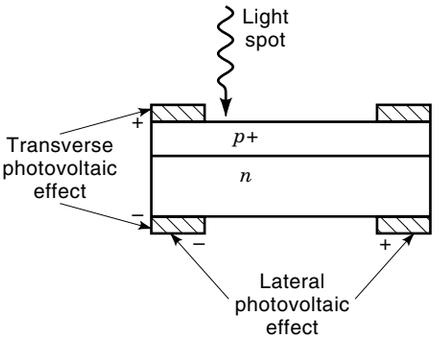

Figure 7. Measurement configurations for the transverse and lateral photovoltaic effects.

where ρ is the resistivity of the p region. If there is no current flow to an external circuit, then outside the illuminated region the transverse current density $J_T(r)$ is given by

$$J_T(r) = J_s(e^{q\varphi(r)/k_b T} - 1) \tag{3}$$

where J_s is the diode saturation current density. Since the change in the lateral current at every point is just equal to the transverse current density at that point, it can be shown that

$$\frac{dJ_L(r)}{dr} = -\frac{J_L(r)}{r} - \frac{J_T(r)}{W} \tag{4}$$

where W is the thickness of the p region. So the variation in the photovoltage $\varphi(r)$ is given by

$$\frac{d^2\varphi(\mathrm{r})}{d^2r} + \frac{1}{r}\frac{d\varphi(\mathrm{r})}{dr} - \frac{\rho J_s}{W}(e^{q\varphi(r)/k_b T} - 1) = 0 \tag{5}$$

Lucovsky solves this equation and extends it to arbitrary geometrical configurations, but his analysis assumes that no current flows through the external contacts, that is, that the value of the lateral photovoltage is sensed without any loading. Connors (5) extends the model further to take account of current flow to an external circuit. He shows that reverse-biasing the junction reduces sensitivity to washout from uniform background illumination superimposed on the light spot. Operating in the fully reverse-biased mode also increases frequency response by increasing the junction depletion region width and thus reducing the capacitance of the photodetector.

Applications

The natural extension of this one-dimensional position-sensitive detector is to add a second pair of contacts to make a two-dimensional position-sensitive detector that can then independently obtain both the x and y coordinates of a light spot. However, the simple addition of another pair of contacts is generally insufficient. While good linearity is demonstrated

for light spot positions directly between a pair of contacts, the response is distorted for off-axis light spots. The distortion can be especially severe when the light spot is near one contact, since it may take most of the photocurrent leaving little for the other contacts. Woltring (6) analyzed the various contact configurations for two-dimensional position-sensitive detectors shown in Fig. 8. Wallmark's original configuration with point contacts at the ends of each axis has rather nonlinear characteristics for off-axis light spots and is rarely used in practice. Duolateral devices exhibit better linearity properties and are commercially available for both optical and nuclear radiation detection. Tetralateral devices are also commercially available. All these devices suffer from nonlinear characteristics near the edges of the device, usually in a pincushion pattern as shown in Fig. 9. One approach recently demonstrated to improve linearity (7) is the use of MOSFETs to connect and disconnect the contacts in turn, alternating between the x-axis pair of contacts and the y-axis pair of contacts. In essence this device is a one-dimensional position-sensitive detector that alternates between the x-axis and the y-axis. At any given moment only one pair of contacts drains the lateral photocurrent, which improves overall linearity by reducing interference from neighboring contacts. This increase in performance comes at the cost of some complexity and reduced speed of operation.

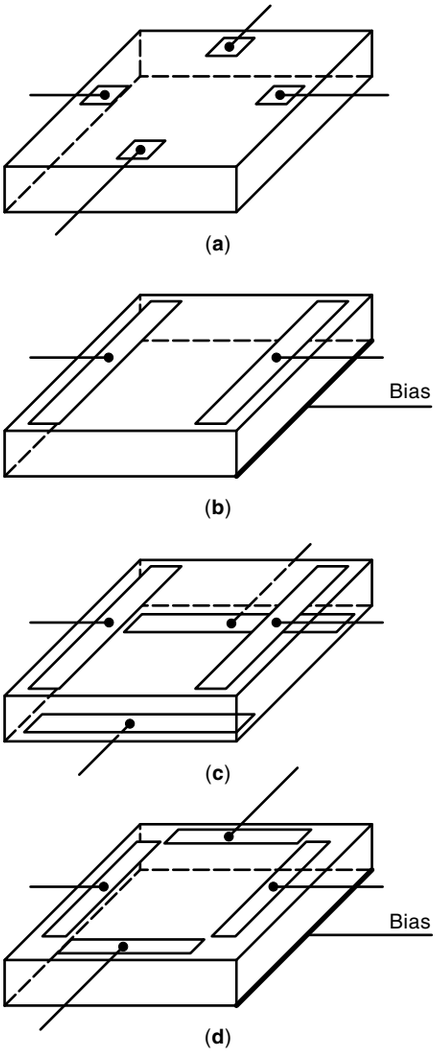

Figure 8. Device configurations for the lateral photovoltaic effect. (a) Dual-axis Wallmark diode. (b) Single-axis duolateral configuration. (c) Dual-axis duolateral configuration. (d) Dual-axis tetralateral configuration.

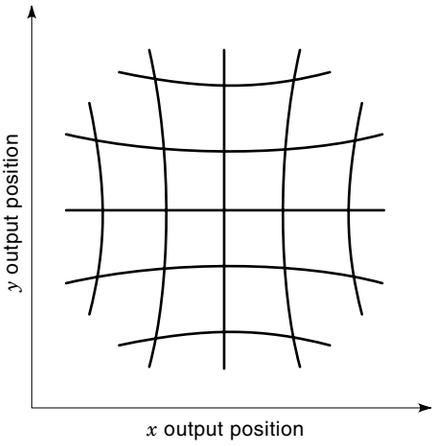

Figure 9. Pincushion distortion typical of some two-dimensional position-sensitive detectors. Lines represent the position output resulting from raster-scanning the detector with a light spot in a square grid pattern.

Figure 10 shows the cross-section of a typical commercial p-type-intrinsic-n-type (PIN) position-sensitive detector based on the lateral photovoltaic effect. This device contains an intrinsic (undoped) layer sandwiched between a p-type layer above and an n-type layer below, and is typically reverse-biased as shown. This device behaves somewhat like an optical potentiometer. Under reverse bias, the nominal relationship between the light spot position and the device output currents is current division between the top layer electrodes, where the light spot position determines the fraction that flows through each electrode. From Fig. 10, if the distance between the electrodes is L and the light spot is a distance x from the first electrode, the current approximately divides as

$$I_1 = I\frac{L-x}{L} \tag{6}$$

and

$$I_2 = I\frac{x}{L} \tag{7}$$

where I_1 and I_2 are the currents through the top electrodes and the total photocurrent through the bottom electrode is $I = I_1 + I_2$. The position of the light spot can be recovered independent of intensity variations by considering the normalized difference $(I_1 - I_2)/I$

$$\frac{I_1 - I_2}{I} = \frac{L-2x}{L} \tag{8}$$

or the ratio I_1/I_2

$$\frac{I_1}{I_2} = \frac{L-x}{x} \tag{9}$$

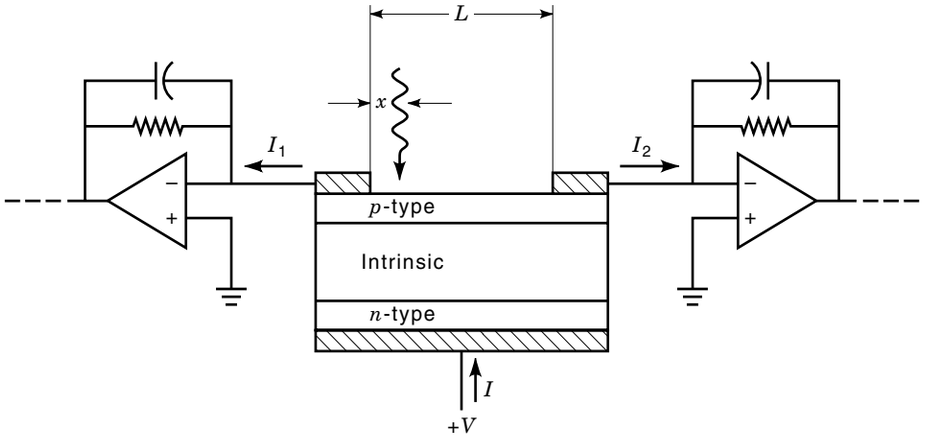

Figure 10. Cross section of 1-D PIN duolateral photodiode with output circuitry. Note the reverse bias held by the $+V$ on the n-layer electrode and the virtual grounds supplied by the operational amplifier circuits connected to the p-layer electrodes.

either of which can be solved for x without any dependence on the incident light intensity. Hamamatsu (8) manufactures silicon one-dimensional position-sensitive detectors, with spectral response 320 nm–1100 nm (ultraviolet through visible and infrared). The Hamamatsu S1352 has a sensitive area 3.4 cm long, with measurement accuracy ± 100 μm in the central region of the device that worsens to ± 500 μm near the edges.

Hamamatsu also manufactures two-dimensional silicon position-sensitive detectors in both duolateral and tetralateral configurations. The equations for the one-dimensional case given previously are applied to each axis for (x, y) outputs. The duolateral Hamamatsu S1300 has an effective area 1.3 cm square with central region accuracy ± 80 μm and a dark current of 300 nA. The tetralateral counterpart Hamamatsu S1200 has the same active area with less central region accuracy (± 150 μm) but it operates at a reduced dark current of just 0.4 nA. The company offers tetralateral position-sensitive detectors with active areas up to 2.7 cm square. They also offer tetralateral devices with a pincushion-shaped active area that achieve central region position accuracies to ± 40 μm. All of these detectors have spectral response 320 nm–1100 nm peaking at 920 nm. The dark current, rise time, and device capacitance generally increase with the size of the active area. Note that the distributed nature of the capacitance and resistance in the detector structure leads to a time constant that varies with the position of the illumination.

Position-sensitive detectors can also detect high energy particles. Some recent inventions incorporating high-energy position-sensitive detectors include: a computerized tomography system for medical imaging; a portable x-ray diffractometer for measurement of stress in metal structures such as pipelines or bridges; an imaging beta tracer microscope; and a method for measuring geological subsidence using radioactive tags previously implanted into a borehole. Hamamatsu manufactures silicon high energy position sensitive detectors that have active areas 8.5 cm in diameter.

Some recently patented applications of optical position-sensitive detectors include: deflection sensors in robotic arm links; laser warning devices that determine the direction of an incident laser beam; camera autofocus elements; position sensors for scanning microscopes; submarine mapping; cantilever position sensors in an atomic force microscope; wafer positioning; document size determination for document readers; and triangulation-based three-dimensional imaging. The lateral photovoltaic effect has also been used to study the homogeneity of semiconductor samples (9). By raster-scanning GaAs/AlGaAs heterostructures with a laser and recording the lateral photovoltage as a function of (x, y) position, it is possible to image material inhomogeneities that affect conductivity, such as cracks and dislocations.

For development work, Hamamatsu and other companies manufacture signal processing boards for interfacing one-dimensional and two-dimensional position-sensitive detectors. Systems that incorporate position-sensitive detectors are routinely available commercially. For example, consider the displacement measurement scheme depicted in Fig. 11 where the displacement of an object is translated into the motion of a light spot on a position-sensitive detector. Keyence Corporation manufactures the LC-2400 series of laser displacement sensors that contain a semiconductor laser for target illumination and a position-sensitive detector to measure target displacement (10). The LC-2420 sensor head has an operating range (distance from sensor to target) of 1 cm $\pm$ 200 μm. When measurements are averaged, displacement resolutions down to 100 Å are claimed. Among the applications for this system are measurements of surface roughage or thickness in a manufacturing setting.

Variations on the basic position-sensitive detector structure are also being investigated for advanced applications. A research group manufacturing semitransparent position-sensitive detectors with a-Si : H films has proposed an angle-sensitive configuration that utilizes one detector stacked directly

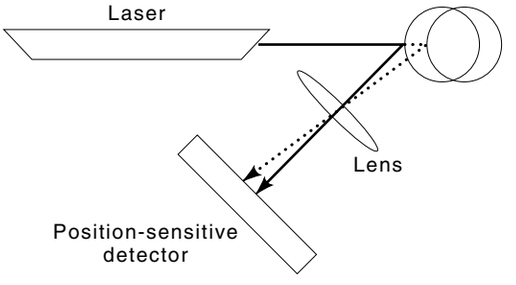

Figure 11. Measurement of displacement using a position-sensitive detector.

atop another (11). Since the distance between the two detectors is known, the difference in position reported by the two detectors can be used to calculate the angle of the incident light. Another group (12) has reported that a resistive crevice down the center of a Ti/Si amorphous superlattice position-sensitive detector enhances the sensitivity within the crevice to 1.5 mV/μm, which can then yield position resolution better than 100 Å.

Porous silicon exhibits a slightly different lateral photovoltaic effect arising from charge trapping at dangling bonds (13). Porous silicon is a network of randomly distributed strands and pores of silicon with dimensions ranging from tens to hundreds of Ångstroms. Researchers have found evidence of quantum confinement effects in these nanoscale silicon structures, including bright visible photoluminescence and electroluminescence, which opens the door for new optoelectronic applications of silicon (14). Porous silicon forms during anodic etching in a hydrofluoric solution, which leaves behind dangling bond traps on the porous surface. Dangling bond traps in silicon are known to be amphoteric, with trapping levels near both the conduction and valence bands. In the case of porous silicon formed from *p*-type silicon, the traps are empty when the material is not illuminated, which makes the upper traps available to trap electrons. When a spot of sufficiently energetic light illuminates this porous silicon, electron-hole pairs are generated. The dangling bonds trap some of the electrons; the rest of the electrons and the photogenerated holes are driven by the widened bandgap of porous silicon into the underlying bulk silicon where they diffuse away and recombine. In steady-state, the electrons trapped in the porous silicon under the light spot cause an electric field directed toward the point of illumination. If the illumination point is located asymmetrically with respect to a pair of lateral contacts, then a lateral photovoltage will develop. The contact nearest the light spot will be negative. The situation for *n*-type is analogous; in this case holes are trapped, resulting in the opposite polarity from that observed for *p*-type. Porous silicon by its porous nature has a large surface to volume ratio, which is important for vapor detectors, and the porous silicon surface is sensitive to changes in the ambient atmosphere. Since this lateral photovoltaic effect provides a direct electrical measurement of the state of dangling bonds in porous silicon, it could be exploited for silicon-based vapor sensors. The generally poor morphology and uniformity are presently preventing porous silicon from industrial use. However, it is found that "gently" etched (15) samples provide much improved morphology and uniformity, qualities important to devices utilizing the lateral photovoltaic effect.

BIBLIOGRAPHY

1. Anonymous, *DPSD Digital Position Sensing Detector,* EG&G Heimann Optoelectronics, sales literature.
2. W. Collins and P. Benfield, The photo-voltaic relay, *Electronic Product Design,* 49–56, May, 1984.
3. Anonymous, *Optoelectronic Designer's Catalog,* Hewlett Packard, 6.265–6.292, June 1993.
4. G. Lucovsky, Photoeffects in nonuniformly irradiated *p-n* junctions. *J. Appl. Phys.,* **31**: 1088–1095, 1960.
5. W. P. Connors, Lateral photodetector operating in the fully reverse-biased mode, *IEEE Trans. Electron Devices,* **ED-18**: 591–596, 1971.
6. H. J. Woltring, Single- and dual-axis lateral photodetectors of rectangular shape, *IEEE Trans. Electron Devices,* **ED-22**: 581–590, 1975.
7. Y. Morikawa and K. Kawamura, A small distortion two-dimensional position-sensitive detector (PSD), *Transducers '91,* 723–726, 1991.
8. Anonymous, *Large-area PSD series,* Hamamatsu Photonics K. K., sales literature, August 1989.
9. P. F. Fontein et al., Use of the lateral photoeffect to study sample quality in GaAs/AlGaAs heterostructures, *J. Appl. Phys.,* **64**: 3085–3088, 1988.
10. Anonymous, *Ultra high accuracy laser displacement sensor: LC-2400A series,* Keyence Corporation of America, sales literature, 1994.
11. S. Arimoto et al., Hydrogenated amorphous silicon position sensitive detector, *J. Appl. Phys.,* **57**: 4778–4782, 1985.
12. R. H. Willens et al., High resolution photovoltaic position sensing with Ti/Si superlattices, *Appl. Phys. Lett.,* **49**: 1647–1648, 1986.
13. D. W. Boeringer and R. Tsu, Lateral photovoltaic effect in porous silicon, *Appl. Phys. Lett.,* **65**: 2332–2334, 1994; expanded version in D. W. Boeringer and R. Tsu, Photovoltaic characterization of trapping in porous silicon, *Mat. Res. Soc. Symp. Proc.,* **358**: 587–592, 1995.
14. K. D. Hirschman et al., Silicon-based visible light-emitting devices integrated into microelectronic circuits, *Nature,* **384**: 338–341, 1996.
15. A. A. Filios, S. S. Hefner, and R. Tsu, Correlation of Raman and optical studies with atomic force microscopy in porous silicon, *J. Vac. Sci. Technol. B,* **B14**: 3431–3435, 1996.

Reading List

K. Zweibel, *Basic Photovoltaic Principles and Methods,* New York, NY: Van Nostrand Reinhold Company Inc., 1984. Very basic introduction to photovoltaics.

J. Fraden, Handbook of Modern Sensors: Physics, Designs, and Applications. 2nd ed., Woodbury, NY: American Institute of Physics, 1997. Exhaustive survey of sensors.

P. Hauptmann, *Sensors: Principles and Applications,* Hertfordshire, England: Prentice Hall, 1993.

R. J. Van Overstraeten and R. P. Mertens, *Physics, Technology, and Use of Photovoltaics.* Bristol, England: Adam Hilger Ltd., 1986.

A. L. Fahrenbruch and R. H. Bube, *Fundamentals of Solar Cells,* New York, NY: Academic Press, Inc., 1983.

S. M. Sze, *Semiconductor Devices, Physics and Technology.* New York: Wiley, 1985. Standard college textbook on solid state devices.

R. H. Bube, *Photoconductivity of Solids.* New York: Wiley, 1960. Thorough treatment of photoconductivity and related processes, including photovoltaic effects.

DANIEL BOERINGER
Northrop Grumman Corporation
RAPHAEL TSU
University of North Carolina at Charlotte

PH-SENSOR. See pH MEASUREMENT AND CONTROL.